ISSN 0915-633X

NATIONAL INSTITUTE FOR FUSION SCIENCE

Direct Observation of Potential Profiles with a 200keV Heavy Ion Beam Probe and Evaluation of Loss Cone Structure in Toroidal Helical Plasmas on the Compact Helical System

A. Fujisawa, H. Iguchi, S. Lee, T.P. Crowley, Y. Hamada, H. Sanuki, K. Itoh, S. Kubo, H. Idei, T. Minami, K. Tanaka, K. Ida, S. Nishimura, S. Hidekuma, M. Kojima, C. Takahashi, S. Okamura and K. Matsuoka

(Received - June 18, 1996)

NIFS-425 July 1996

RESEARCH REPORT
NIFS Series

NAGOYA, JAPAN

Direct Observation of Potential Profiles with a 200keV Heavy Ion Beam Probe and Evaluation of Loss Cone Structure in Toroidal Helical Plasmas on the Compact Helical System

A. Fujisawa, H. Iguchi, S. Lee, T. P. Crowley [1], Y. Hamada
H. Sanuki, K. Itoh, S. Kubo, H. Idei, T. Minami, K. Tanaka, K. Ida,
S. Nishimura, S. Hidekuma, M. Kojima, C. Takahashi, S. Okamura, K. Matsuoka

National Institute for Fusion Science
Furo-cho, Chikusa-ku, Nagoya, 464-01, Japan

Abstract

This paper presents direct experimental observations of potential profiles of a toroidal helical plasma in the Compact Helical System, using a 200keV heavy ion beam probe. Electron cyclotron heated plasmas show a positive potential profile in a low density regime ($\bar{n}_e = 3 \times 10^{12}\text{cm}^{-3}$), while neutral beam injection heated plasmas ($\bar{n}_e = 8 \times 10^{12}\text{cm}^{-3}$) exhibit a negative potential profile. A loss cone structure evaluated from the observed potential is discussed to understand the behavior of high energy particle in a toroidal helical plasma.

Keywords: Potential Profile, Electric Field Profile, Loss Cone Structure, Heliotron/Torsatron Device, Heavy Ion Beam Probe

[1] Rensselaer Polytechnic Institute, Troy, New York, U. S. A.

Rotational transform of vacuum magnetic field configurations is an advantage of toroidal helical plasmas for realization of a steady state fusion reactor. However, the helical ripples inherent with such magnetic field structure give birth to large deviation of high energy particle orbits from the magnetic f ux surface[1], and it will result in deterioration of confinement property and heating efficiency in a collisionless regime. Particularly, the loss cone regime is larger in such devices with a small aspect ratio which is superior from an economical point of view[2]. Plasma potential is a key physics quantity to affect the loss cone structure by inducing an $E \times B$ motion to helically trapped particles.

Even in tokamaks, the discoveries of the H-mode[3] or other improved confinement modes stimulate interests in an internal electric field or potential structure which should be associated with the phase transition[4]. The potential profiles were measured in the ISX-B and the TEXT tokamaks with a heavy ion beam probe (HIBP) [5, 6]. In toroidal helical devices, complicated beam trajectories have prevented from easy measurements of potential profiles with HIBPs. Direct measurements of accurate potential profile are, however, significantly important in a toroidal helical device to investigate the effects of the loss cone structure and the electric field shear on the confinement properties.

The first application of the HIBP measurements, using a traditional method[7], were performed on ECH plasmas of the Advanced Toroidal Facility (ATF) torsatron. In the Compact Helical System[8], which is a heliotron/torsatron device with a low aspect ratio, the radial electric field has been deduced from plasma rotation velocity using a Charge Exchange Recombination Spectroscopy (CXS) [9, 10]. Recently, a 200keV HIBP has been constructed with a new idea to manage complicated probing beam trajectories, which is termed *active trajectory control*[11, 12]. With this method,

we have succeeded to measure radial profiles of electrostatic potentials (or electric fields) in the CHS plasmas, covering over the whole plasma region within a short period (a few ms) of a discharge. In this letter. we will present the potential profiles of electron cyclotron (ECH) and low density neutral beam injection (NBI) heated plasmas. and will discuss relationship between a loss cone structure and potential, and their roles on heating efficiency and confinement property of high energy particles.

The Compact Helical System (CHS) is a heliotron/torsatron device whose major radius is $R_0 = 1.0$m, and averaged minor radius is $\bar{a} = 0.2$m; hence the aspect ratio is $R/\bar{a} = 5$. The CHS has a pair of helical winding coils and four pairs of poloidal coils to control position and shape of the plasma. The magnetic field configuration has a periodicity of $l = 2$ and $m = 8$ in poloidal and toroidal directions, respectively. The potential measurements here were performed in the magnetic configuration whose magnetic axis was located on 0.921m, and its magnetic field strength was 0.9T. In the present experiments, the neutral beam was injected tangentially and the 53GHz gyrotron was used. The working gas and the injected neutral beam are both hydrogen.

In potential measurements with HIBPs, a singly charged heavy ion beam (primary beam) is injected into a target plasma, and then doubly charged ions created with an electron impact ionization (secondary beam) come out with the energy change corresponding to the plasma potential at the ionization point. In case of toroidal helical devices, the secondary beams coming from different observation points may be widely distributed in entrance positions and angles at the energy analyzer. This problem causes a restriction of observation range and energy measurement errors due to an uncertainty in the beam injection angle. An introduction of secondary beam sweep system gives the following advantages to the CHS HIBP; (1) a wider observation range, (2) reduction in the energy measurement errors, and (3) allowance for

the energy analyzer location with a sufficient distance from the plasma to avoid UV loading and leakage magnetic field.

The observation points are illustrated in Fig. 1a when a 72keV cesium beam is used for the magnetic field configuration whose axis is located on $R_{\rm ax} = 92.1$cm. The points in the figure are the projections obtained by tracing a magnetic field line from the actual observation points, whose toroidal angles are shown in Fig.1b, where $\zeta = 0°$ means a toroidal position of vertically elongated f ux surfaces. The points are distributed along the toroidal direction in about a half of the helical pitch (45°). The beam trajectories for the observation points are confirmed to lead secondary beams into the energy analyzer properly in gas ionization experiments[12]. The error caused by an uncertainty in the beam injection angle into the analyzer is estimated to be within 10V[12].

Figure 2a demonstrates potential profiles obtained during steady states of ECH and NBI plasmas. The open and closed circles indicate the potential profiles of ECH plasmas with low ($\bar{n}_e = 3 \times 10^{12}$cm^{-3}) and medium density ($\bar{n}_e = 8 \times 10^{12}$cm^{-3}), respectively. The central electron temperatures of the low and medium density cases are $T_e(0) = 900$eV, $T_e(0) = 400$eV, respectively. The squares indicate the potential profile of a co-injected NBI plasma where the electron density is $\bar{n}_e = 8 \times 10^{12}$cm^{-3}, and the electron and ion temperatures are $T_e(0)$=300eV, $T_i(0)$=200eV, respectively. These profiles are averages for about 20ms of steady states, and the error bars mean standard deviations.

The potential is positive with the center value of about 200 V for a low density ECH plasma where electrons are almost in a collisionless regime since the electron collisionality is $\nu_e^*(\bar{a}/2) = 1.4$. The definition of the collisionality here is $\nu^*(r) = \nu_{\rm eff}(r)/\omega_{\rm b}(r)$ with $\nu_{\rm eff} = \nu/\epsilon_{\rm h}$ and $\omega_{\rm b} = \iota(\epsilon_{\rm h}T/m)^{1/2}/2\pi R$, where ι is the rotational transform. In the medium density ECH plasma,

the potential exhibits an interesting characteristic; the electric field is positive around core, while it has a large negative value ($\simeq$ 70V/cm) near the edge. The electron collisionality is $\nu_e^*(\bar{a}/2) = 13.1$, and the electron is in the plateau regime. On the other hand, the potential in the low density NBI plasma is negative with the center value of about -200 V. The collisionalities of electrons and ions are $\nu_e^*(\bar{a}/2) = 6.0$, $\nu_i^*(\bar{a}/2) = 8.2$, respectively. The electrons and ions are both in the plateau regime.

Figure 2b shows radial electric field profiles deduced from polynomial fitting curves to the obtained potential profiles. In the ECH plasmas, a tendency can be seen that the positive electric field turns more negative as the density increases. In the medium density case, the electric field exhibits a strong negative field around the plasma edge although the statistical error bar is large. In the NBI case, the ion temperature, electron density and temperature profiles are available from the data base. Hence, the experimental electric field can be compared with the electric field predicted with the ambipolarity condition $\Gamma_{\rm i}(E_{\rm r}) = \Gamma_{\rm e}(E_{\rm r})$, where $\Gamma_{\rm i}(E_{\rm r})$ and $\Gamma_{\rm e}(E_{\rm r})$ represent the electron and ion f uxes in the neoclassical theory, respectively[13-15]. A dashed-dotted line in Fig. 2b represents a neoclassical radial electric field for the NBI plasma. The expected electric field is quantitatively consistent with the experimental result in this case.

In toroidal plasmas, important roles of the radial electric field on confinement (e.g., absolute trapping of particles, the reduction in turbulence, or heating efficiency) have been discussed. In toroidal helical plasmas, the electric field has a significant effect on helical trapped particle orbits whose guiding center motion is expressed by $\mathrm{d}\theta/\mathrm{d}t = V_\perp \cos\theta/r + \omega_{\rm E\times B} + \omega_{\nabla B}$, where θ, $V_\perp$, $\omega_{\rm E\times B}$ and $\omega_{\nabla B}$ represent the poloidal angle, the toroidal drift velocity, the rotation angular velocities due to $E \times B$ and ∇B drifts, respectively. Here, the definitions are $V_\perp = \varepsilon_{\rm t} W/qBr$, $\omega_{E\times B} = E/Br$, $\omega_{\nabla B} = \varepsilon_{\rm h} W/qBr^2$,

with W and q being the energy and the charge, respectively. If the resonance condition $\omega_{\mathrm{ExB}} + \omega_{\nabla B} \simeq 0$ (or $W \simeq -q\phi/\varepsilon_{\mathrm{h}}$) is satisfied, the helical trapped particles run away from the plasma owing to the toroidal drift. Then a loss cone will spread over the plasma.

An analytical formula was given to evaluate the loss cones for electrons and ions[13, 16] when the potential profile is a monotonically decreasing or increasing function. The loss cone for deeply trapped particles is expressed as $W_{\mathrm{m}} < W < W_{\mathrm{p}}$, where W is the particle energy, and $W_{\mathrm{m}} = -q\phi(0)f(x)/(\epsilon_{\mathrm{ha}}(1-x^2) + \epsilon_{\mathrm{ta}}(1-x))$, $W_{\mathrm{p}} = -q\phi(0)f(x)/(\epsilon_{\mathrm{ha}}(1-x^2) - \epsilon_{\mathrm{ta}}(1+x))$. Here, ϵ_{ta} and ϵ_{ha} represent toroidal and helical ripple coefficients, respectively, and x indicates the horizontal coordinate whose origin is on the magnetic axis, and $f(x)$ is a normalized function fitted to the experimental profiles with $f(0) = 1$, $f(\pm 1) = 0$. A loss cone of deeply trapped ions for the NBI plasma using the observed negative potential profile is shown in Fig. 3a, where we choose $\epsilon_{\mathrm{ta}} = 0.16$ and $\epsilon_{\mathrm{ha}} = 0.255$. The loss cone plays a role when the helically trapped particles can accomplish their one-turn orbits poloidaly without a collision. This criterion is roughly expressed as $\omega_{\nabla B} > \nu/\epsilon_{\mathrm{h}}$. Figure 3a plots the critical energy W_{rot} to satisfy the criterion which is explictly written as $W_{\mathrm{rot}}^{2.5}(eV) > 1.4 \times 10^{-2} n_{\mathrm{e}}(\mathrm{cm}^{-3}) B(T) r(\mathrm{cm})^2 \varepsilon_{\mathrm{h}}^{-1}$. This criterion is no longer valid around the magnetic axis since there the banana width is larger than the local structure owing to the small poloidal field.

When the NBI is injected into this plasma, the energy transfer rates to ions and electrons are a function of electron temperature. The beam energy to heat ions and electrons equally is represented by $W_{\mathrm{p_i=p_e}} = 15 T_e A_{\mathrm{b}} [Z_{\mathrm{i}}^2/A_{\mathrm{i}}]^{2/3}$, where A_{b}, A_{i} and Z_{i} are the atomic mass of the beam particles, the atomic mass and the charge of the bulk plasmas, respectively. Above this energy ($\sim 15 T_{\mathrm{e}}$), the beam particles heat selectively electrons, preserving the pitch angle. On the other hand, the injected beam particles experience pitch angle

scatterings in the region below this energy, transferring their energy to ions. It becomes, therefore, more probable for the beam particles to enter into the loss cone below this energy.

The neutral beam is tangentially injected in the CHS with the energy about 35 keV (the hatched region in Fig. 3a). The energy transfer from injected beams to bulk ions occurs effectively in the regime between the upper loss cone boundary and the energy of $W_{\mathrm{p_i=p_e}}(= 15Te)$. As for the bulk ions, the ion temperature is below the lower loss cone boundary, the bulk ions are confined by the rotation due to $E \times B$ motion. If the potential becomes sufficiently negative for the loss cone region to be located above the energy of $W_{\mathrm{p_i=p_e}}$, the ion heating efficiency will be improved since the pitch angle scatterings occur below the loss cone region.

We can also demonstrate a loss cone region for deeply trapped electrons for the low density ECH plasma with a positive potential. It is shown in Fig. 3b that the loss cone region above the energy of W_{rot} exists only in the outside($x > 0$). The critical energy W_{rot} for electrons is higher than that for ions since the collision frequency is larger for the same energy; $W_{\mathrm{rot}}^{2.5}(eV) > 6.3\times10^{-1} n_{\mathrm{e}}(\mathrm{cm}^{-3}) B(T) r(\mathrm{cm})^2 \varepsilon_{\mathrm{h}}^{-1}$. Thus, the electron heated up by the wave on the outside of torus will easily enter into the loss cone. As for ions, the loss cone region in this positive potential is localized only in an outside periphery of the plasma. The loss cone boundary is shown by the dashed line in Fig. 3b. The similar dashed line in Fig. 3a shows the loss cone for electrons in the NBI plasma.

This fact suggests that a scenario to realize a hot ion mode is possible if a positive potential profile can be kept in an NBI-heated plasma with an effective use of ECH. The heating efficiencies for electrons and ions in toroidal helical plasmas can be ameliorated or deteriorated by the state of electrostatic potential. Actually, in the Wendelstein VII-A (WVII-A) experiments high

ion confinement was attained in discharges with a strong negative potential generated with perpendicular NBI heating[17]. On the other hand, a recent discovery of a high ion temperature mode in the Heliotron-E plasma was suggested to be related to the strong electric field shear[18].

The present profile measurements over the whole plasma region made it possible to find an unique spatial structure of the electric field profile in the medium density ECH plasma; positive electric field changes negative gradually from the core to the edge. The strong shear of the electric field around the edge seen in Fig. 2b allows us to evaluate the possible impact on the turbulent suppression. The theory based on stabilization of the interchange instability suggests that the strong shear may result in reduction in f uctuation driven transport by a few percents[19]. At the level of plasma heating ($\sim$ 100kW), the turbulent suppression is expected to be marginal.

Efforts have been made on the CHS to evaluate the radial electric field with the CXS measurements[9, 10]. The deduced electric field profile in a similar NBI heated plasma presented here ($\bar{n}_e = 6.5 \times 10^{12}\mathrm{cm}^{-3}$) indicated $E_r = 0 \pm 10\mathrm{V/cm}$. The error bar arises from the fact that the amount of photon was limited in that density region. The HIBP shows that the electric field profile of the NBI plasma is negative, which is clearly different from that in the ECH plasma of a similar electron density.

The momentum balance equation $\nabla P_\alpha = eZ_\alpha n_\alpha(\vec{E} + \vec{v}_\alpha \times \vec{B}) + \vec{R}_\alpha$ is used in the evaluation of the radial electric field from the impurity rotation velocity, with assumptions that the friction force $\vec{R}_\alpha = 0$. Here, P_α, Z_α, n_α and v_α are the pressure, the charge, the density and the velocity of the impurity identified by α, respectively. In higher electron density regime ($n_e > 2 \times 10^{13}\mathrm{cm}^{-3}$), presently stronger UV radiation from the plasma affects the power supplies of secondary beam sweep system. After the applicable region of the HIBP is extended to higher density discharges by reinforcing

the power supply capacity, simultaneous measurements of electric field profiles (HIBP) and impurity velocities (CXS) will allow to estimate this friction force working on impurities, and give a new insight to impurity transports.

In summary, we have measured directly internal potential profiles in a toroidal helical plasma of the CHS heliotron/torsatron, using an HIBP with a newly proposed beam control method. The potential profiles show a clear difference in the ECH and NBI plasmas which exhibit electron (positive electric field) and ion roots (negative electric field) characteristics, respectively. Comparison is made between theoretical and experimental electric fields for a low density NBI case. The consistency shown in this case needs further investigation to examine whether it is valid for other operational conditions; different temperature and density regimes, and so on. Improved confinement modes of a low aspect toroidal helical plasma can be achieved by controlling the loss cone structure through the potential profile. Therefore, it is a future work for the HIBP measurements to clarify a physical mechanism of potential formation for exploration of improved confinement regimes in toroidal helical plasmas.

Acknowledgements

The authors are very grateful to Dr. M. Fujiwara for his continuous encouragements. The authors also acknowledge useful discussions with Dr. S-I. Itoh. The acknowledgements are given to the CHS experimental group for their cooperation.

References

[1] B. B. Kadomtsev, O. P. Pogutse, Nucl. Fusion **11**, 67(1971).

[2] B. A. Carreras, N. Dominguez, L. Garcia, *et al.*, Nucl. Fusion **28** 1195(1988).

[3] ASDEX Team, Nucl. Fusion **29** 1959(1989).

[4] K. Itoh, S-I. Itoh, Phys. Contr. Fusion **38**, 1(1996).

[5] G. A. Hallock, J. Mathew, W. C. Jennings *et al.*, Phys. Rev. Lett. **56** 1248(1986).

[6] X. Z. Yang, B. Z. Zhang, A. J. Wootton, *et al.*, Phys. Fluids B **3** 3448(1991).

[7] S. C. Aceto, J. G. Schwelberger *et al.*, *in Proceedings of International Conference on Plasma Physics, Innsbruck, 1992*, Vol. 16C, Pt. I, P.. 529.

[8] K. Matsuoka, S. Kubo, M. Hosokawa et al., *in Plasma Physics and Controlled Nuclear Fusion Research 1988* (Proc. 12th Int. Conf. Nice, 1988), Vol. 2., IAEA Vienna(1989) 411.

[9] K. Ida, H. Yamada, H. Iguchi, S. Hidekuma, H. Sanuki, K. Yamazaki, Phys. Fluids B **3**, 515(1991).

[10] H. Idei, K. Ida, H. Sanuki *et al.*, Phys. Rev. Lett. **71** 2220(1993).

[11] A. Fujisawa, H. Iguchi, M. Sasao, Y. Hamada, J. Fujita, Rev. Sci. Instrum. **63** 3694(1992).

[12] A. Fujisawa, H. Iguchi, S. Lee *et al.*, NIFS Report-415. To be published to Rev. Sci. Instrum.

[13] H. Sanuki, K. Itoh, S-I. Itoh, J. Phys. Soc. Jpn. **62**. 123(1993).

[14] D. E. Hastings, W. A. Houlberg, K. C. Shaing, Nucl. Fusion **25** 445(1985).

[15] L. M. Kovrizhnykh, Nucl. Fusion **24**, 435(1984).

[16] K. Itoh, S-I. Itoh *et al.*, Nucl. Fusion **29** 1851(1989).

[17] H. Wobig, H. Maassberg, H. Renner, The WVII-A Team, the ECRH Group and the NI Group, *in Plasma Physics and Controlled Nuclear Fusion Research*, (Proc. 11th Int. Conf. Kyoto,1986), Vol. 2, IAEA, Vienna(1987)369.

[18] K. Ida, K. Kondo, K. Nagasaki, T. Hamada *et al.*, Phys. Rev. Lett. **76** 1268(1996).

[19] K. Itoh, S-I. Itoh, A. Fukuyama, H. Sanuki and M. Yagi, Plasma Phys. Control. Fusion **36** 123(1994).

Figure Captions

Fig. 1: (A) Observation points projected onto a horizontal elongated cross-section of magnetic f ux surfaces in case of a magnetic field configuration with the axis location of 92.1cm. (B) Toroidal angle from the vertically elongated cross-section of the actual observation points.

Fig. 2: (A) Potential profiles measured with a 200keV HIBP. The open and closed circles represent potential profiles of low ($\bar{n}_e = 3 \times 10^{12}\text{cm}^{-3}$) and medium density ($\bar{n}_e = 8 \times 10^{12}\text{cm}^{-3}$) ECH plasmas, respectively. The squares are the potential profile of a low density tangentially co-injected NBI plasma ($\bar{n}_e = 8 \times 10^{12}\text{cm}^{-3}$). (B) Radial electric field profiles deduced from the potential profiles. The dotted-dashed line represents an electric field predicted from a theory for the low density NBI heated plasma case.

Fig. 3: The evaluated loss cone for deeply trapped ions in a low density NBI heated plasma using the negative potential profile measured with the HIBP; $\phi(0) = -200\text{V}$. The dashed line W_{rot} means the ion energy at which the ion can accomplish poloidaly one-turn orbits. The dotted-dashed line $W_{\text{pi=pe}}$ represents that energy transfer from high energy ion beam to the bulk electrons and ions occurs equally. The loss cone boundary for deeply trapped electrons is also indicated by the other dashed line. The circles are the ion temperature measured with a CXR system. (B) The evaluated loss cone for deeply trapped electrons in low density ECH plasma where the positive potential with $\phi(0) = 200\text{V}$ is observed. The loss cone boundary for deeply trapped ions is also indicated by a dashed line. The open circles are the electron temperature measured with a Thomson scattering system.

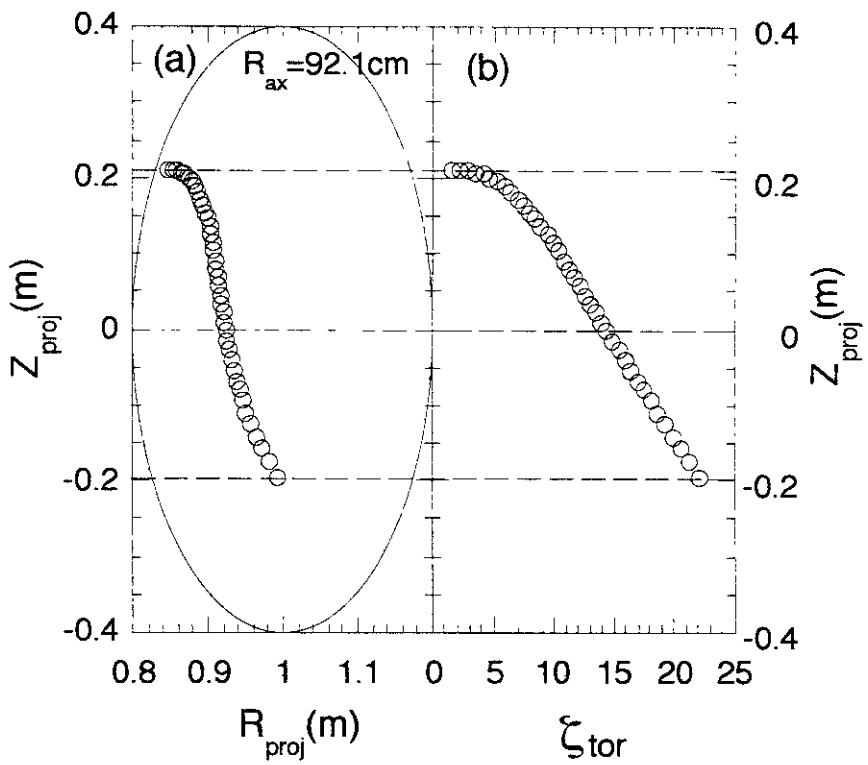
(a)
R_ax=92.1cm
(b)
0.4
0.2
0
-0.2
-0.4
Z_proj(m)
0.8 0.9 1 1.1
R_proj(m)
0 5 10 15 20 25
ζ_tor

Figure 1

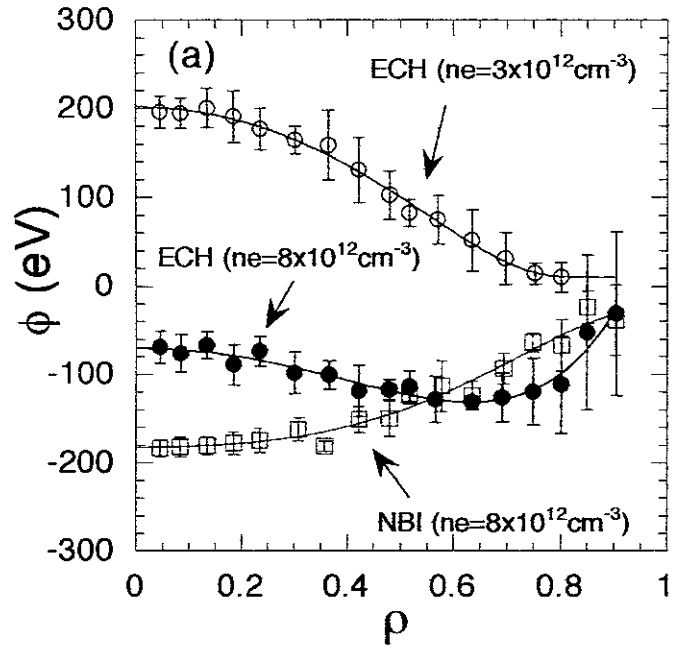
(a)
ECH (ne=3x10^12cm^-3)
ECH (ne=8x10^12cm^-3)
NBI (ne=8x10^12cm^-3)
ϕ (eV)
ρ
300
200
100
0
-100
-200
-300
0
0.2
0.4
0.6
0.8
1

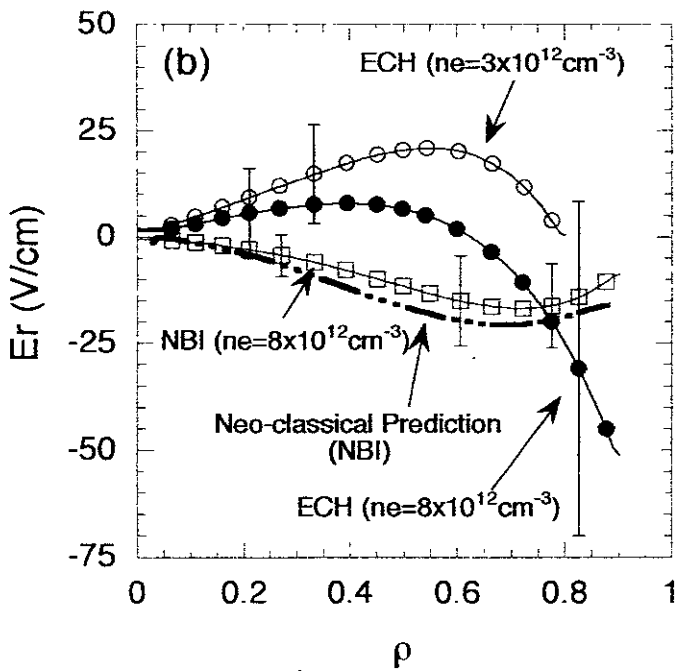
(b)
ECH (ne=3x10^12cm^-3)
NBI (ne=8x10^12cm^-3)
Neo-classical Prediction
(NBI)
ECH (ne=8x10^12cm^-3)
Er (V/cm)
ρ
50
25
0
-25
-50
-75
0
0.2
0.4
0.6
0.8
1

Figure 2

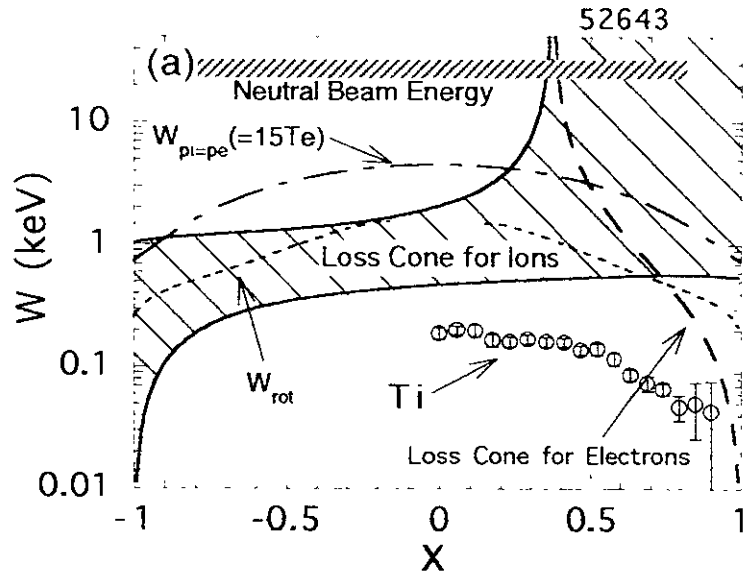
52643
(a)
Neutral Beam Energy
$W_{pi=pe}$(=15Te)
Loss Cone for Ions
W_{rot}
Ti
Loss Cone for Electrons
W (keV)
10
1
0.1
0.01
-1
-0.5
0
0.5
1
X

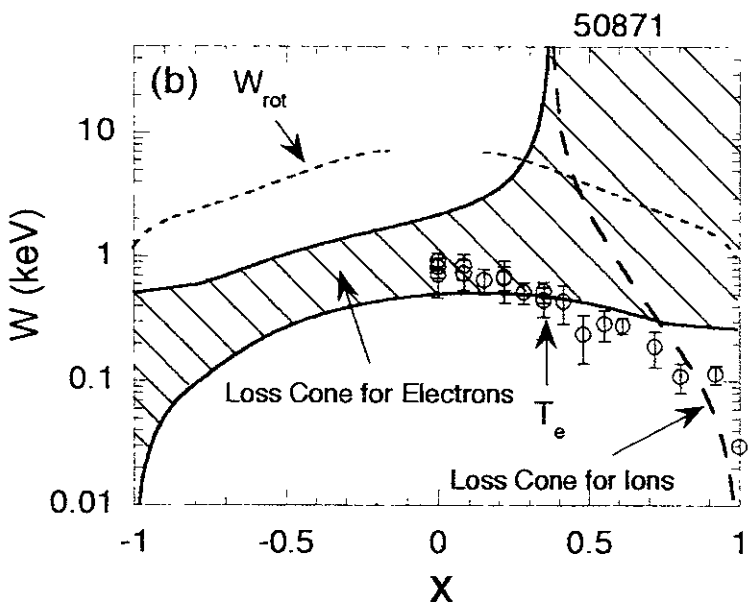
50871
(b)
W_{rot}
Loss Cone for Electrons
T_e
Loss Cone for Ions
W (keV)
10
1
0.1
0.01
-1
-0.5
0
0.5
1
X

Figure 3

Recent Issues of NIFS Series

NIFS-379 H. Shimazu, S. Machida and M. Tanaka,
Macro-Particle Simulation of Collisionless Parallel Shocks; Oct. 1995

NIFS-380 N. Kondo and Y. Kondoh,
Eigenfunction Spectrum Analysis for Self-organization in Dissipative Solitons; Oct. 1995

NIFS-381 Y. Kondoh, M. Yoshizawa, A. Nakano and T. Yabe,
Self-organization of Two-dimensional Incompressible Viscous Flow in a Friction-free Box; Oct. 1995

NIFS-382 Y.N. Nejoh and H. Sanuki,
The Effects of the Beam and Ion Temperatures on Ion-Acoustic Waves in an Electron Beam-Plasma System; Oct. 1995

NIFS-383 K. Ichiguchi, O. Motojima, K. Yamazaki, N. Nakajima and M. Okamoto
Flexibility of LHD Configuration with Multi-Layer Helical Coils;
Nov. 1995

NIFS-384 D. Biskamp, E. Schwarz and J.F. Drake,
Two-dimensional Electron Magnetohydrodynamic Turbulence; Nov. 1995

NIFS-385 H. Kitabata, T. Hayashi, T. Sato and Complexity Simulation Group,
Impulsive Nature in Collisional Driven Reconnection; Nov. 1995

NIFS-386 Y. Katoh, T. Muroga, A. Kohyama, R.E. Stoller, C. Namba and O. Motojima,
Rate Theory Modeling of Defect Evolution under Cascade Damage Conditions:The Influence of Vacancy-type Cascade Remnants and Application to the Defect Production Chracterization by Microstructural Analysis; Nov. 1995

NIFS-387 K. Araki, S. Yanase and J. Mizushima,
Symmetry Breaking by Differential Rotation and Saddle-node Bifurcation of the Thermal Convection in a Spherical Shell; Dec. 1995

NIFS-388 V.D. Pustovitov,
Control of Pfirsch-Schlüter Current by External Poloidal Magnetic Field in Conventional Stellarators: Dec. 1995

NIFS-389 K. Akaishi,
On the Outgassing Rate Versus Time Characteristics in the Pump-down of an Unbaked Vacuum System; Dec. 1995

NIFS-390 K.N. Sato, S. Murakami, N. Nakajima, K. Itoh,
Possibility of Simulation Experiments for Fast Particle Physics in Large Helical Device (LHD); Dec. 1995

NIFS-391 W.X.Wang, M. Okamoto, N. Nakajima, S. Murakami and N. Ohyabu,
A Monte Carlo Simulation Model for the Steady-State Plasma in the Scrape-off Layer; Dec. 1995

NIFS-392 Shao-ping Zhu, R. Horiuchi, T. Sato and The Complexity Simulation Group,
Self-organization Process of a Magnetohydrodynamic Plasma in the Presence of Thermal Conduction; Dec. 1995

NIFS-393 M. Ozaki, T. Sato, R. Horiuchi and the Complexity Simulation Group
Electromagnetic Instability and Anomalous Resistivity in a Magnetic Neutral Sheet; Dec. 1995

NIFS-394 K. Itoh, S.-I Itoh, M. Yagi and A. Fukuyama,
Subcritical Excitation of Plasma Turbulence; Jan. 1996

NIFS-395 H. Sugama and M. Okamoto, W. Horton and M. Wakatani,
Transport Processes and Entropy Production in Toroidal Plasmas with Gyrokinetic Eletromagnetic Turbulence; Jan. 1996

NIFS-396 T. Kato, T. Fujiwara and Y. Hanaoka,
X-ray Spectral Analysis of Yohkoh BCS Data on Sep. 6 1992 Flares - Blue Shift Component and Ion Abundances -; Feb. 1996

NIFS-397 H. Kuramoto, N. Hiraki, S. Moriyama, K. Toi, K. Sato, K. Narihara, A. Ejiri, T. Seki and JIPP T-IIU Group,
Measurement of the Poloidal Magnetic Field Profile with High Time Resolution Zeeman Polarimeter in the JIPP T-IIU Tokamak; Feb. 1996

NIFS-398 J.F. Wang, T. Amano, Y. Ogawa, N. Inoue,
Simulation of Burning Plasma Dynamics in ITER; Feb. 1996

NIFS-399 K. Itoh, S-I. Itoh, A. Fukuyama and M. Yagi,
Theory of Self-Sustained Turbulence in Confined Plasmas; Feb. 1996

NIFS-400 J. Uramoto,
A Detection Method of Negative Pionlike Particles from a H2 Gas Descharge Plasma; Feb. 1996

NIFS-401 K.Ida, J.Xu, K.N.Sato, H.Sakakita and JIPP TII-U group,
Fast Charge Exchange Spectroscopy Using a Fabry-Perot Spectrometer in the JIPP TII-U Tokamak; Feb. 1996

NIFS-402 T. Amano,
Passive Shut-Down of ITER Plasma by Be Evaporation; Feb. 1996

NIFS-403 K. Orito,
A New Variable Transformation Technique for the Nonlinear Drift Vortex; Feb. 1996

NIFS-404 T. Oike, K. Kitachi, S. Ohdachi, K. Toi, S. Sakakibara, S. Morita, T. Morisaki, H. Suzuki, S. Okamura, K. Matsuoka and CHS group; *Measurement of Magnetic Field Fluctuations near Plasma Edge with Movable Magnetic Probe Array in the CHS Heliotron/Torsatron*, Mar. 1996

NIFS-405 S.K. Guharay, K. Tsumori, M. Hamabe, Y. Takeiri, O. Kaneko, T. Kuroda, *Simple Emittance Measurement of H- Beams from a Large Plasma Source*; Mar. 1996

NIFS-406 M. Tanaka and D. Biskamp, *Symmetry-Breaking due to Parallel Electron Motion and Resultant Scaling in Collisionless Magnetic Reconnection*; Mar. 1996

NIFS-407 K. Kitachi, T. Oike, S. Ohdachi, K. Toi, R. Akiyama, A. Ejiri, Y. Hamada, H.Kuramoto, K. Narihara, T. Seki and JIPP T-IIU Group, *Measurement of Magnetic Field Fluctuations within Last Closed Flux Surface with Movable Magnetic Probe Array in the JIPP T-IIU Tokamak*; Mar. 1996

NIFS-408 K. Hirose, S. Saito and Yoshi.H. Ichikawa *Structure of Period-2 Step-1 Accelerator Island in Area Preserving Maps*; Mar. 1996

NIFS-409 G.Y.Yu, M. Okamoto, H. Sanuki, T. Amano, *Effect of Plasma Inertia on Vertical Displacement Instability in Tokamaks*; Mar. 1996

NIFS-410 T. Yamagishi, *Solution of Initial Value Problem of Gyro-Kinetic Equation*; Mar. 1996

NIFS-411 K. Ida and N. Nakajima, *Comparison of Parallel Viscosity with Neoclassical Theory*; Apr. 1996

NIFS-412 T. Ohkawa and H. Ohkawa, *Cuspher, A Combined Confinement System*; Apr. 1996

NIFS-413 Y. Nomura, Y.H. Ichikawa and A.T. Filippov, *Stochasticity in the Josephson Map*; Apr. 1996

NIFS-414 J. Uramoto, *Production Mechanism of Negative Pionlike Particles in H_2 Gas Discharge Plasma*; Apr. 1996

NIFS-415 A. Fujisawa, H. Iguchi, S. Lee, T.P. Crowley, Y. Hamada, S. Hidekuma, M. Kojima, *Active Trajectory Control for a Heavy Ion Beam Probe on the Compact Helical System*; May 1996

NIFS-416 M. Iwase, K. Ohkubo, S. Kubo and H. Idei
Band Rejection Filter for Measurement of Electron Cyclotron Emission during Electron Cyclotron Heating; May 1996

NIFS-417 T. Yabe, H. Daido,T. Aoki, E. Matsunaga and K. Arisawa,
Anomalous Crater Formation in Pulsed-Laser-Illuminated Aluminum Slab and Debris Distribution; May 1996

NIFS-418 J. Uramoto,
Extraction of K^- Mesonlike Particles from a D_2 Gas Discharge Plasma in Magnetic Field; May 1996

NIFS-419 J. Xu, K. Toi, H. Kuramoto, A. Nishizawa, J. Fujita, A. Ejiri, K. Narihara, T. Seki, H. Sakakita, K. Kawahata, K. Ida, K. Adachi, R. Akiyama, Y. Hamada, S. Hirokura, Y. Kawasumi, M. Kojima, I. Nomura, S. Ohdachi, K.N. Sato
Measurement of Internal Magnetic Field with Motional Stark Polarimetry in Current Ramp-Up Experiments of JIPP T-IIU; June 1996

NIFS-420 Y.N. Nejoh,
Arbitrary Amplitude Ion-acoustic Waves in a Relativistic Electron-beam Plasma System; July 1996

NIFS-421 K. Kondo, K. Ida, C. Christou, V.Yu.Sergeev, K.V.Khlopenkov, S.Sudo, F. Sano, H. Zushi, T. Mizuuchi, S. Besshou, H. Okada, K. Nagasaki, K. Sakamoto, Y. Kurimoto, H. Funaba, T. Hamada, T. Kinoshita, S. Kado, Y. Kanda, T. Okamoto, M. Wakatani and T. Obiki,
Behavior of Pellet Injected Li Ions into Heliotron E Plasmas; July 1996

NIFS-422 Y. Kondoh, M. Yamaguchi and K. Yokozuka,
Simulations of Toroidal Current Drive without External Magnetic Helicity Injection; July 1996

NIFS-423 Joong-San Koog,
Development of an Imaging VUV Monochromator in Normal Incidence Region; July 1996

NIFS-424 K. Orito,
A New Technique Based on the Transformation of Variables for Nonlinear Drift and Rossby Vortices; July 1996

NIFS-425 A. Fujisawa, H. Iguchi, S. Lee, T.P. Crowley, Y. Hamada, H. Sanuki, K. Itoh, S. Kubo, H. Idei, T. Minami, K. Tanaka, K. Ida, S. Nishimura, S. Hidekuma, M. Kojima, C. Takahashi, S. Okamura and K. Matsuoka,
Direct Observation of Potential Profiles with a 200keV Heavy Ion Beam Probe and Evaluation of Loss Cone Structure in Toroidal Helical Plasmas on the Compact Helical System; July 1996